Version of November 15, 2004

Comparison of Chandra and XMM spectra of galaxy clusters

Massimiliano Bonamente

NASA NSSTC, Huntsville, Alabama

Physics Department, The University of Alabama in Huntsville, John Wright Dr., OB201, Huntsville, Alabama, 35899

bonamem@.uah.edu

1. XMM data reduction

Use SAS xmmsas_20040318_1831-6.0.0, CCF files dated > Dec 11 2003.

1. Emchain and epchain pipelines run on the raw odf data from the XMM archive:
emchain withbadpix=yes badpixfindalgo=EM rejectbadevents=no
epchain withbadpix=yes withbadpixfind=yes keeprejected=yes

2. Filters applied:
MOS: pattern<=12 and flag=0
PN: pattern=0 and flag=0

3. Light curves extracted for the full field of view, to check the presence of 'flares'.
MOS: Light curves extracted at E>9.5 keV, in 500 s bins (see Table).
PN: Likewise, only that light curves are extracted at E>10 keV.

4. Spectra extracted. Use the light curves above to filter out time intervals when flares are present, so that the count rate in high-energy band is similar to the quiescent count rate (see Table).

5. Arf files generated with arfgen, appropriate .rfm files used from the SAS archive.

6. Background used is the blank-sky files from D. Lumb. Background event files are filtered in the same manner as the cluster observation: same filters (point 2. above) and

same light curve criteria (point 3. and 4. above). Background spectra are extracted at the same (X,Y) coordinates as the cluster observation, after reprojecting the blank-sky files with the attcalc tool.

2. Chandra data reduction

Use CIAO 3.1, CALDB v. 2.28 (also CIAO 3.0.1, CALDB 2.26 for comparison).

1. Run acis_process_events on the Level 1 events file from Chandra archive. CTI correction applied, latest GAIN file applied. [1]

2. Select events with grade=0,2,3,4,6 and status=0, and apply the standard GTI file from the Chandra archive.

3. Light curve in 0.5-5 keV from a region free of celestial sources, to check the presence of flares. Mean count rate calculated for the entire light curve, and exclude time intervals $> 4\sigma$ (no such occurrence present in these 4 clusters).

4. Use acisspec to extract spectra and generate .arf and .rmf files. Low-energy correction for ACIS-S3 contaminant applied by the mkwarf tool. [2] Spectra are binned to have at least 25 counts in each channel, and further rebinned at low energy in order to reduce the statistical noise.

5. Background used is from the blank-sky datasets provided with the CIAO software. Dataset used is the closest in time to the cluster observation, same GAIN file applied to this dataset as to the cluster observation. Background spectra are extracted at the same (X,Y) coordinates as the cluster observation, after reprojecting the blank-sky file with the reproject_events tool.

3. Data analysis

For each cluster, I extracted one spectrum. I chose the 2-4 arcmin annulus for AS1101, A3112 and A1795, in order to avoid the central 'cooling' region, and the full ACIS-S3 field for Coma, covering a $\sim 8\times$ arcmin^{-2} area. Model is WABS*MEKAL in XSPEC, Galactic

[1] The latest time-dependent PHA drift correction is not applied, as it has virtually no effect for S3 (I checked on A1795).

[2] The ardlib parameter AXAF_ACIS_CONTAM_FILE = CALDB applies the correction.

Table 1. XMM and Chandra cluster data

Cluster	XMM obs.	Obs date	Filter	Livetime	Chandra obs.	Obs. date	Livetime
AS1101	0147800101	2002-11-20	Thin1	120 ks	1668	2001-08-13	10 ks
A3112	0105660101	2000-12-24	Medium	23 ks	2216	2001-05-24	7 ks
					2515	2001-09-12	17 ks
A1795	0097820101	2000-06-26	Thin1	50 ks	3666	2002-06-10	15 ks
Coma	0124711401	2000-05-29	Medium	20 ks	1086	1999-11-04	10 ks

Table 2. XMM and Chandra analysis information

Cluster	MOS1		MOS2		PN		ACIS-S3 Exp.
	c/r limits	Exp.	c/r limits	Exp.	c/r limits	Exp.	
AS1101	71-108	68.7 ks	75-112	66.8 ks	112-168	64.2 ks	10 ks
A3112	71-108	20.8 ks	75-112	20.3 ks	112-168	15.3 ks	7.2 ks
							16.9 ks
A1795	0-150	29.7 ks	0-150	13.3 ks	0-210	19.2 ks	14.4 ks
Coma	71-108	13.8 ks	75-112	14.8 ks	112-168	10.8 ks	9.5 ks

Note. — XMM: c/r limits on light curve, in 500 s bins, PN: PI > 10000; MOS: PI > 9500. Light curve is extracted from the whole field of view. *A1795: higher limits used.* Chandra: Light curve is extracted in energy=500-5000 (0.5-5 keV) from a peripheral region of the observation without sources, in 500 s bins. Excluded times are those that exceed the mean by 4 sigma. There are no excluded intervals in these three clusters, light curves are rather flat.

N_H was fixed at the Dickey and Lockman survey value (AS1101: 1.8 $\times 10^{20}$ cm^{-2}, A3112: 2.6 $\times 10^{20}$ cm^{-2}, A1795: 1.0 $\times 10^{20}$ cm^{-2}, Coma: 0.9 $\times 10^{20}$ cm^{-2}). The normalization constant of the MEKAL model is the same for the two MOS instruments.

All error bars are 90% confidence ($\chi^2_{min} + 2.7$ for 1 interesting parameter), unless otherwise specified. Gaussian errors were assumed in the spectral data (although the default in CIAO 3.1 is Poisson error, errors were recalculated as $\sqrt{(NCOUNTS)}$ in each channel, before rebinning).

3.1. Fit to 2-7 keV band

Results of the 2-7 keV fit are shown in Table 3. Chandra and XMM temperature and abundances agree well for all clusters, except for A1795, where the agreement is marginal. The low-energy residuals, however, are in strong disagreement. Notice the 1-2 keV depletion in the Chandra data, instead of the the soft excess in the XMM instruments.

.

Table 3. 2-7 keV fit

Cluster	MOS1 + MOS2 + PN			ACIS-S3, v.2.26			ACIS-S3, v.2.28			ACIS-S3, v.2.28, calcarf		
	kT (keV)	A (solar)	χ^2_r (dof)	kT (keV)	A (solar)	χ^2_r (dof)	kT (keV)	A (solar)	χ^2_r (dof)	kT (keV)	A (solar)	χ^2_r (dof)
AS1101	2.86±0.1	0.19±0.04	1.39(190)	$2.82\pm^{0.69}_{0.41}$	$0.39\pm^{0.39}_{0.30}$	0.85(72)	$3.09\pm^{0.75}_{0.53}$	$0.33\pm^{0.35}_{0.28}$	0.83(72)		same	
A3112	$5.13\pm^{0.35}_{0.29}$	0.33±0.05	1.19(189)	$4.83\pm^{1.06}_{0.77}$	$0.36\pm^{0.21}_{0.19}$	0.83(85)	$6.8\pm^{0.9}_{0.8}$	$0.51\pm^{0.14}_{0.13}$	0.98(279)		same	
A1795	6.85±0.25	0.28±0.03	1.12(190)	$5.82\pm^{0.60}_{0.44}$	0.21±0.07	1.05(131)	$6.2\pm^{0.6}_{0.5}$	0.19±0.07	0.94(110)		same	
Coma	8.87±0.21	0.25±0.02	1.31(189)	$9.15\pm^{0.94}_{0.74}$	0.16±0.07	1.03(130)	$8.52\pm^{0.74}_{0.71}$	0.11±0.06	1.23(131)	$8.9\pm^{0.8}_{0.7}$	0.11±0.06	1.23(132)

3.2. Fit to 1-7 keV band

Results of the 1-7 keV fit are shown in Table 4. The XMM fits are typically unacceptable, because of positive residuals at energies ~1-1.5 keV. Temperature and abundances are at variance between the Chandra and XMM instruments, the differences are attributable to the 1-2 keV band. There is a systematic trend, whereby the Chandra temperatures are higher than XMM's.

Ettori et al. (2002) measures $\sim$ 6.4±0.5 keV from the 2-3' annulus of Coma, using the same Chandra data.

4. Comparison with PKS2155-304 XMM data

I analyzed the XMM data of PKS2155-304, same dataset analyzed in Kaastra et al. (2003). Galactic N_H was fixed at 1.36 $\times 10^{20}$ cm$-$2. The observation suffers from pile-up, but this problem was resolved by choosing only an annular region of the detector, away from the center of the detected emission. I used the task epatplot to check that pile-up was not a problem with this extraction region.

I fit the PN and MOS2 data separately first. Residuals in the low-energy band are shown in the figures. It seems that fitting 2-7 keV region alone leaves some low-energy residuals in PN (the residuals are negative in MOS). In fact, the PN residuals in clusters are always larger than in MOS. The different fits (0.3-7 keV, 1-7 keV and 2-7 keV) give consistent results for the best fit power-law parameters.

Then I fit the PN and MOS2 together, mimicking what is done for cluster spectra. Again, the fits give consistent results, and the 2-7 keV fit gives positive residuals that are respectively +5% and +6% for MOS2 and PN in the 0.3-1 keV band, and $\sim$ 0% in the 1-2 keV band.

5. Comparison with other data

I also compare the ACIS results with other data available from the literature.

In addition, I compare the global temperatures obtained by the latest CALDB 2.28 data with ASCA temperatures for other galaxy clusters.

Table 4. 1-7 keV fit

Cluster	MOS1 + MOS2 + PN			ACIS-S3 v. 2.26			ACIS-S3 v. 2.28			ACIS-S3 v. 2.28,calcarf		
	kT (keV)	A (solar)	χ_r^2 (dof)	kT (keV)	A (solar)	χ_r^2 (dof)	kT (keV)	A (solar)	χ_r^2 (dof)	kT (keV)	A (solar)	χ_r^2 (dof)
AS1101	2.53±0.04	0.25±0.02	1.78(254)	$3.04\pm^{0.28}_{0.27}$	$0.35\pm^{0.15}_{0.13}$	0.85(96)	3.19±0.28	$0.36\pm^{0.16}_{0.13}$	0.81(95)	2.99±0.25	0.35±0.14	0.84(97)
A3112	4.51±0.12	0.34±0.04	1.27(253)	$5.52\pm^{0.52}_{0.48}$	$0.43\pm^{0.19}_{0.18}$	0.98(108)	$7.3\pm^{0.53}_{0.38}$	0.62±0.14	1.21(372)	7.1±0.4	0.62±0.13	1.22(372)
A1795	5.86±0.10	0.28±0.02	1.43(254)	6.43±0.31	0.30±0.07	1.28(155)	$7.10\pm^{0.32}_{0.32}$	0.25±0.08	1.29(134)	6.8±0.3	0.26±0.07	1.31(134)
Coma	7.74± ∼0.15	0.25± ∼0.02	2.58(253)	$9.22\pm^{0.42}_{0.38}$	0.15±0.07	1.34(153)	9.00±0.38	0.10±0.06	1.40(154)	$9.4\pm^{0.5}_{0.4}$	0.11±0.06	1.40(156)

Note. — Redshift was a fit parameter for A3112 ($z = 0.070\pm^{0.0023}_{0.0032}$) and Coma (z=$0.018\pm^{0.002}_{0.001}$). For Coma, the result is different from the nominal redshift o $z = 0.023$. A3112: the CALDB 2.26 results are only for OBSID 2216. A3112: observatins studied by Takizawa 2003, ApJ 595 142, finds kT about 6 keV at 2 arcmin

Table 5. PKS2155-304 XMM fits – separate MOS2 and PN fits

0.3-7 keV fit		1-7 keV fit		2-7 keV fit	
α	χ^2_r(dof)	α	χ^2_r(dof)	α	χ^2_r(dof)
			MOS2		
2.78±0.007	1.31(327)	2.79±0.016	1.27(281)	2.82±0.05	1.16 (206)
			PN		
2.802±0.005	1.12(761)	2.77±0.015	0.98(621)	2.71±0.04	0.95(419)

Table 6. PKS2155-304 XMM fits – joint MOS2/PN fit

α	Norm. MOS2	Norm. PN	χ^2_r(dof)
	0.3-7 keV fit		
2.793±0.004	0.0341±0.0001	0.0248±0.0001	1.23(1085)
	2-7 keV fit		
2.760±0.030	0.033±0.001	0.024±0.001	1.03(626)

Table 7. Comparison with other data

Cluster	ASCA	BeppoSAX	Ginga	Other XMM analyses
Coma	9±0.6 (D99: <9')	9.2±0.4, 10.0±0.4 (D01: 0-2, 2-4')	8.2±0.2 (H93: $\sim$ 1 deg)	8.25±0.1 (A01: <10')
				7.3±1 (K04: 2-4')
A1795	8±1.5 (M98, 2-6')	6.2±0.2 (D01: 2-4')		6±0.3 (A01b: 2-4')
				6±0.2 (T01: 2-4')
				5.6±0.3 (K04: 2-4')
A3112	6±1.5, 3±1.5 (M98: 0-6', 6-19')			4.1±0.4 (K04: 2-4')
	6±1 (W00: 2-10')			
AS1101				2.4±0.1 (K04: 2-4')

Note. —
D01: De Grandi et al. 2002, ApJ 567, 163
H93: Hughes et al. 1993, ApJ, 404, 61
M98: Markevitch et al. 1998, ApJ, 503, 77
A01: Arnaud et al. 2001, A&A, 365, L67
D99: Donnelly et al. 1999, ApJ, 513, 690
A01b: Arnaud et al. 2001, A&A 365, L80
T01: Tamura et al. 2001, A&A 365, L87
K04: Kaastra et al. 2004, A&A, 413, 415
W00: White 2000, MNRAS, 312, 663

Table 8. Comparison of global temperatures for other selected clusters

Cluster	Chandra (CALDB 2.28)	Chandra (CALDB 2.28 calcarf)	ASCA	XMM	Chandra lit
Cl0016+1609	11.6±1	10.3±0.9	8.9±0.6 (H04)	9.1±0.2 (WB03)	
			7.6±0.7 (HB98)		
			7.5±0.8 (W00)		
A68					
A267					
A370	8.8±0.5	8.8± 0.8	6.6±0.6 (098)		
			5.7±0.6 (W00)		
MS0451-0305	10.7±1	10.3± 1	$10.3\pm^{0.9}_{0.8}$ (H04)		10.2±1 (D03)
MACS0647+7015					
A586	7.4±0.7	6.6±0.6	6±0.6 (W00)		
MACS0744+3927					
A611	7.0±0.3	6.8±0.5	6.6±0.6 (HPC)		
A665	9.6±0.6	7.3±0.4	7.7±0.4 (W00)		8.2±0.5 (G04)
A697	12.0±0.8	9.9±1	8.6±0.5 (W00)		
A773	9.0±0.8	$7.5\pm^{0.8}_{0.5}$	8.6±0.7 (W00)		7.5±0.8 (G04)
Zw3146	7.2±0.2	6.6±0.3	5.9±0.3 (W00)		
MACS1115+5320					
MS1137+6625	5.6±0.6	5.2±0.8	$9.5\pm^{2.8}_{2}$ (H04)		
			$5.7\pm^{2}_{1}$ (D99)		
MACS1149+2223					
A1413	8.2±0.3	7.3±0.3	7.3±0.3 (W00)	6.9±0.2 (PA02)	
			6.6±0.5 (I02)		
			6.7±0.3 (M01)		
CL1226+33	14.1±2	$12.6\pm^{4}_{2.6}$	11.5±2 (M04)	$12.6\pm^{3}_{2.2}$ (M04)	
MACS1311-0310					
A1689	11.9±0.5	10.0±0.6	9.2±0.3 (W00)	9.3±0.2 (AM04)	9.1±0.9 (X02)
RXJ1347-1145	15.6±0.6	13.4±0.8	12.9±0.9 (AF98)		12.2±0.6 (A02)

098: Ota et al. 1998, ApJ, 495, 170
W00: White 2000, MNRAS, 312, 663
HPC: Hughes, private comm.
D99: Donahue et al. 1999, ApJ, 527, 525
AF98: Allen and Fabian 1998a, MNRAS, 297, L57
P00: Patel et al. 2000, Apj, 541, 37
WB03: Worrall and Birkinshaw 2003, MNRAS, 340, 1261
H04: Henry 2004, ApJ, 609, 603
P01: Pratt, Arnaud and Aghanim, 2001, Moriond meeting proceedings
PA02: Pratt and Arnaud 2002, A&A 394, 375
I02: Ikebe et al. 2002, A&A 383, 773
M01: Matsumoto et al. 2001, PASJ 52, 153
M02: Majerowicz et al. 2002, A&A 394, 77
M04: Maughan et al. 2004, MNRAS 351, 1193
A02: Allen et al. 2002, MNRAS 335, 256
S97: Schindler et al. 1997, A&A 317, 646
G04: Govoni et al. 2004, ApJ 605, 695
D03: Donahue et al. 2003, Apj 598, 190
X02: Xue et al. 2002, Apj, 576, 152
AM04: Anderson and Madejski 2004, ApJ, 607, 190
CL0016: XMM temperature fit to 0.4-10 keV
A2163: XMM temp fit to 0.5-10 keV, 1.65e+21 NH
A1413: XMM temp. fit to 0.3-10 keV
A1835: XMM temp. fit to 0.3-10 keV
A1689: XMM temp. fit to 0.3-10 keV (PN¿1 keV)
RXJ1347: Chandra lit. fit to 0.5-7 keV
A2163: Chandra lit. fit with variable N_H

Table 8—Continued

Cluster	Chandra (CALDB 2.28)	Chandra (CALDB 2.28 calcarf)	ASCA	XMM	Chandra lit
			$11.8\pm^{1.6}_{1}$ (S97)		
MS1358	8.7±0.7	8.2±1	7.5±0.5 (AF98)		
A1835	8.4±0.2	8.4±0.4	7.9±0.5 (W00)	7.6±0.4 (M02)	
MACS1423+2404					
A1914	12.1±0.5	9.9±0.5	10.5±0.5 (W00)		10.9±0.7 (G04)
A1995	8.9± 0.4	8.6±0.6	7.6±0.9 (W00)		
			8.6±0.8 (P00)		
A2111					
A2163	15.1±0.4	16.4±1.1	13.3±0.6 (W00)	14.6±0.9 (P01)	12.4±0.7 (G04)
A2204	6.7±0.2	6.5±0.3	7.0±0.2 (W00)		
A2218	9.5±0.5	8.2±0.6	6.8±0.3 (W00)		6.7±0.5 (G04)
RXJ1716+6708					
A2259					
A2261	8.8±0.8	7.1±0.7	7.5±0.5 (W00)		
			8.8±0.4 (AF98)		
MS2053.7-0449	5.2±0.5	$4.6\pm^{0.9}_{0.7}$	$8.1\pm^{3.7}_{2.2}$ (H04)		
MACS2129-0741					
RXJ2129+0005					
MACS2214-1359					
MACS2228+2036					
MACS2243.3-0935					

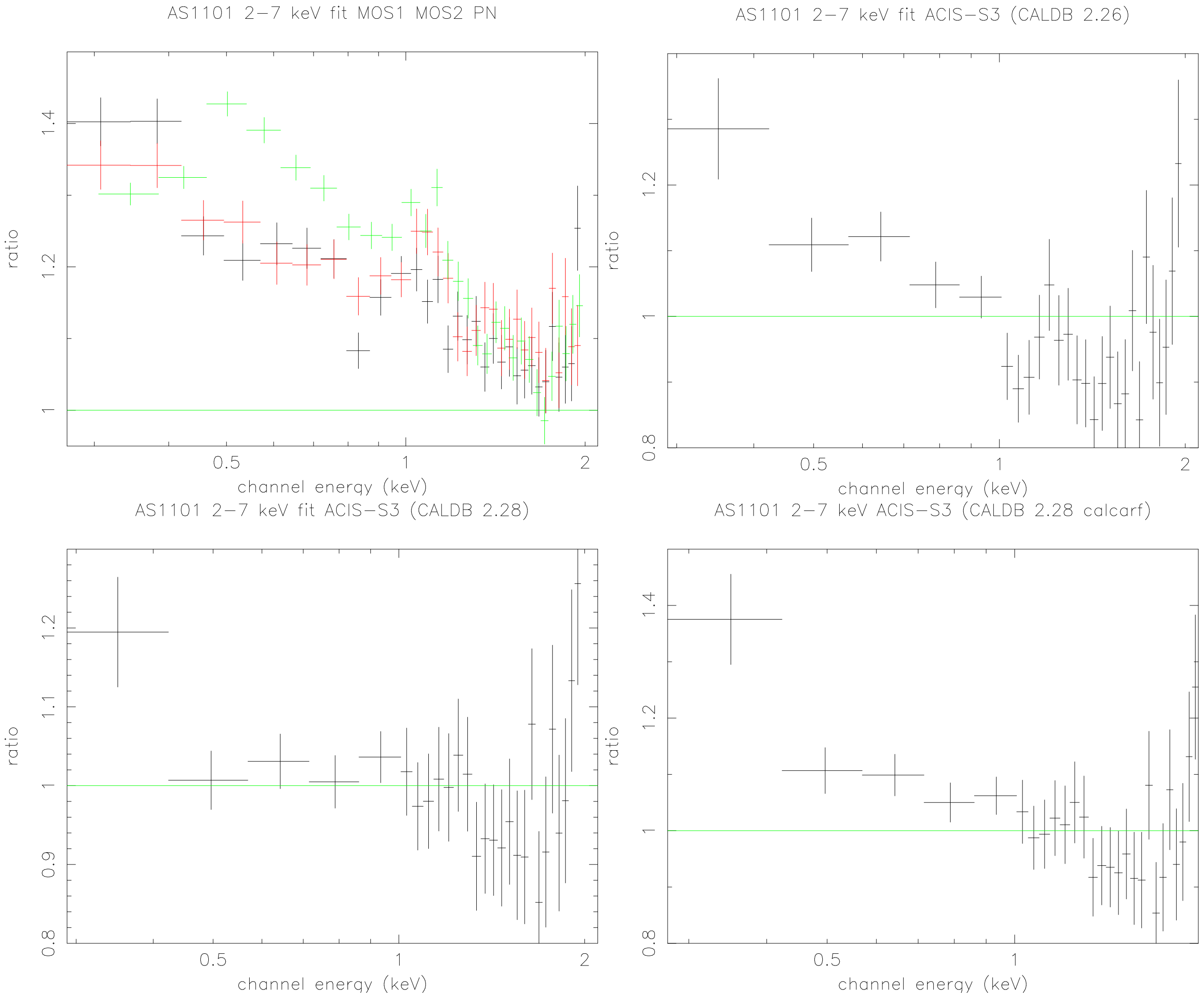

Fig. 1.— AS1101, 2-7 keV fit results

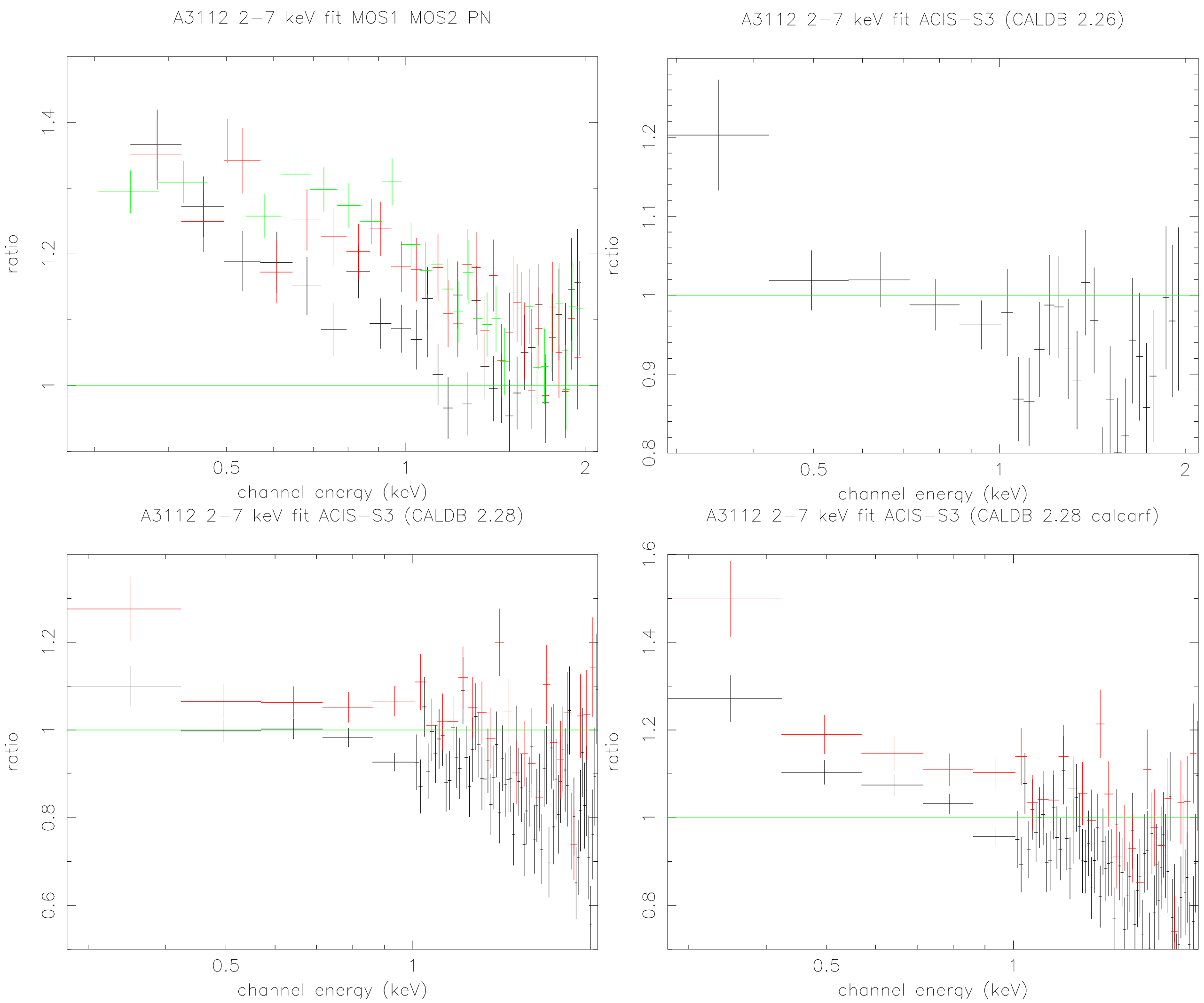

Fig. 2.— A3112, 2-7 keV fit results

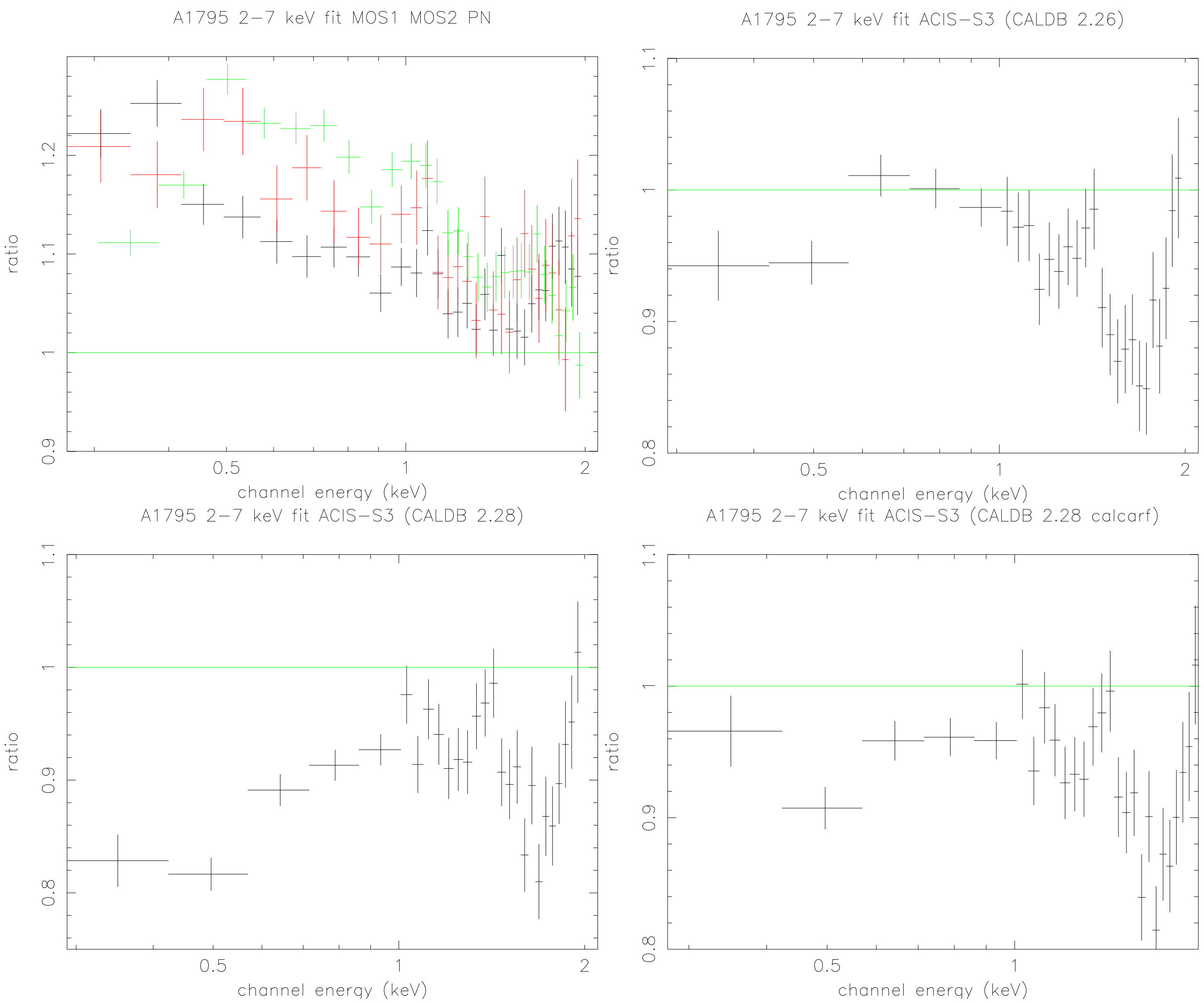

Fig. 3.— A1795, 2-7 keV fit results

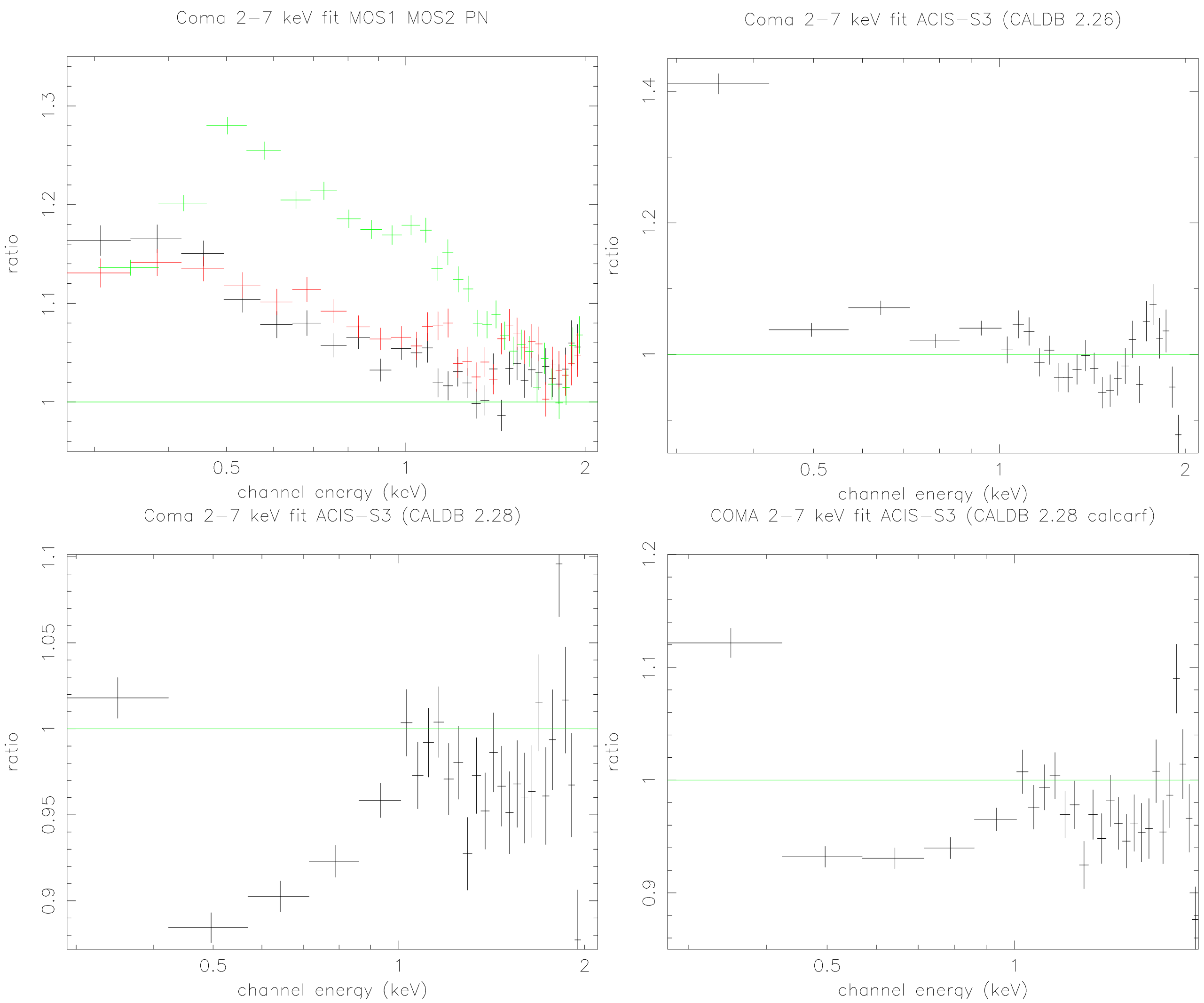

Fig. 4.— Coma cluster, 2-7 keV fit results

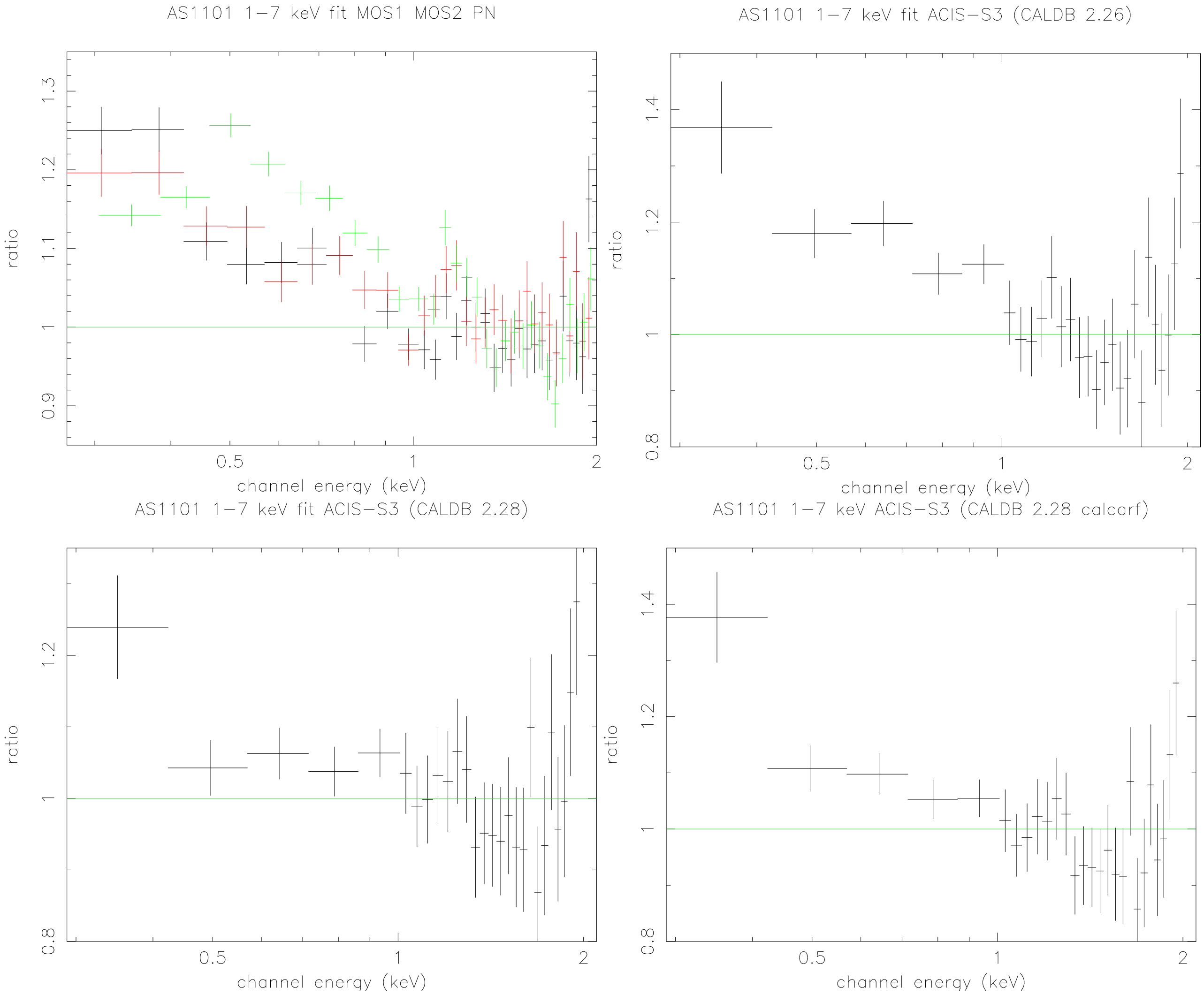

Fig. 5.— AS1101, 1-7 keV fit results

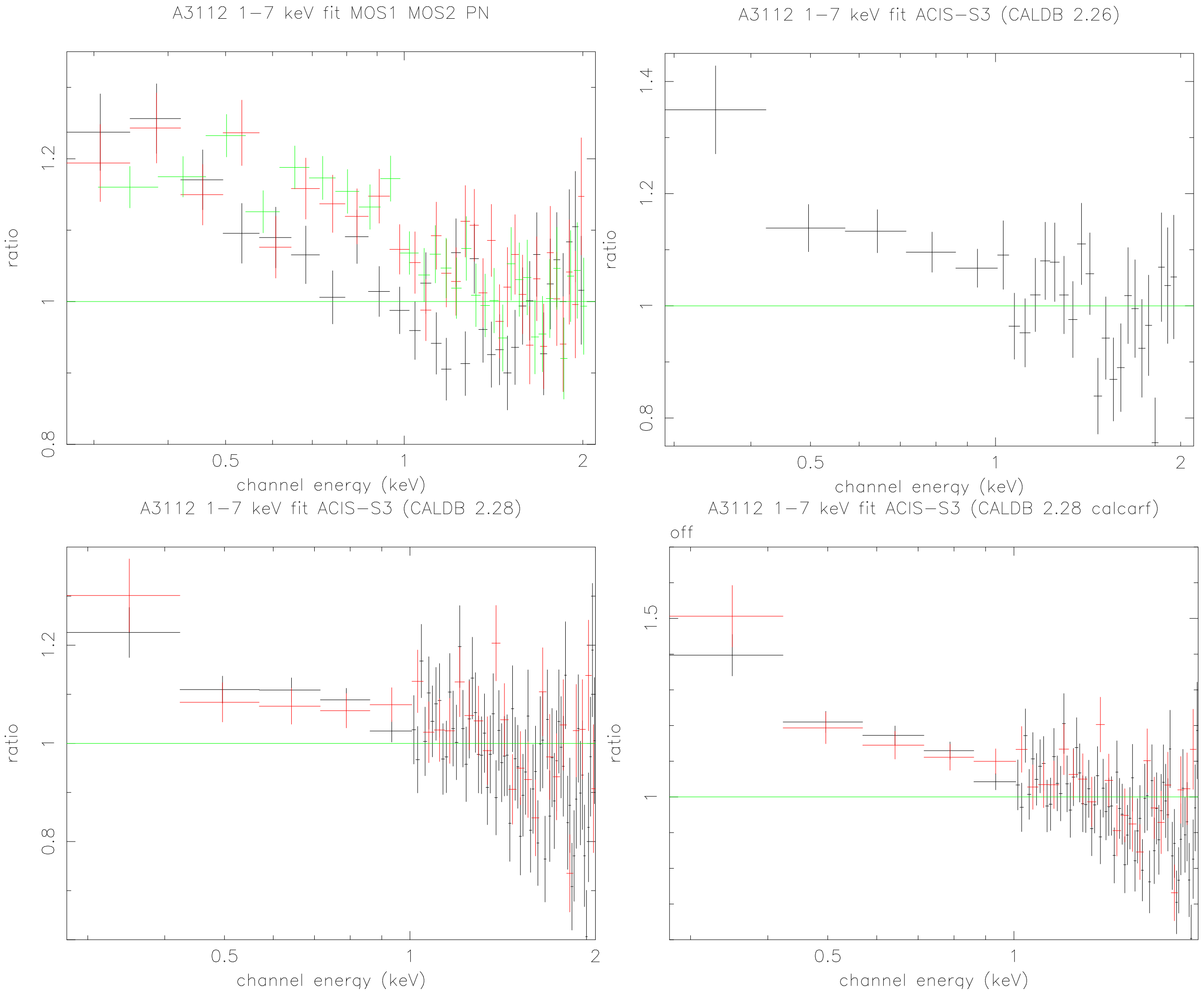

Fig. 6.— A3112, 1-7 keV fit results

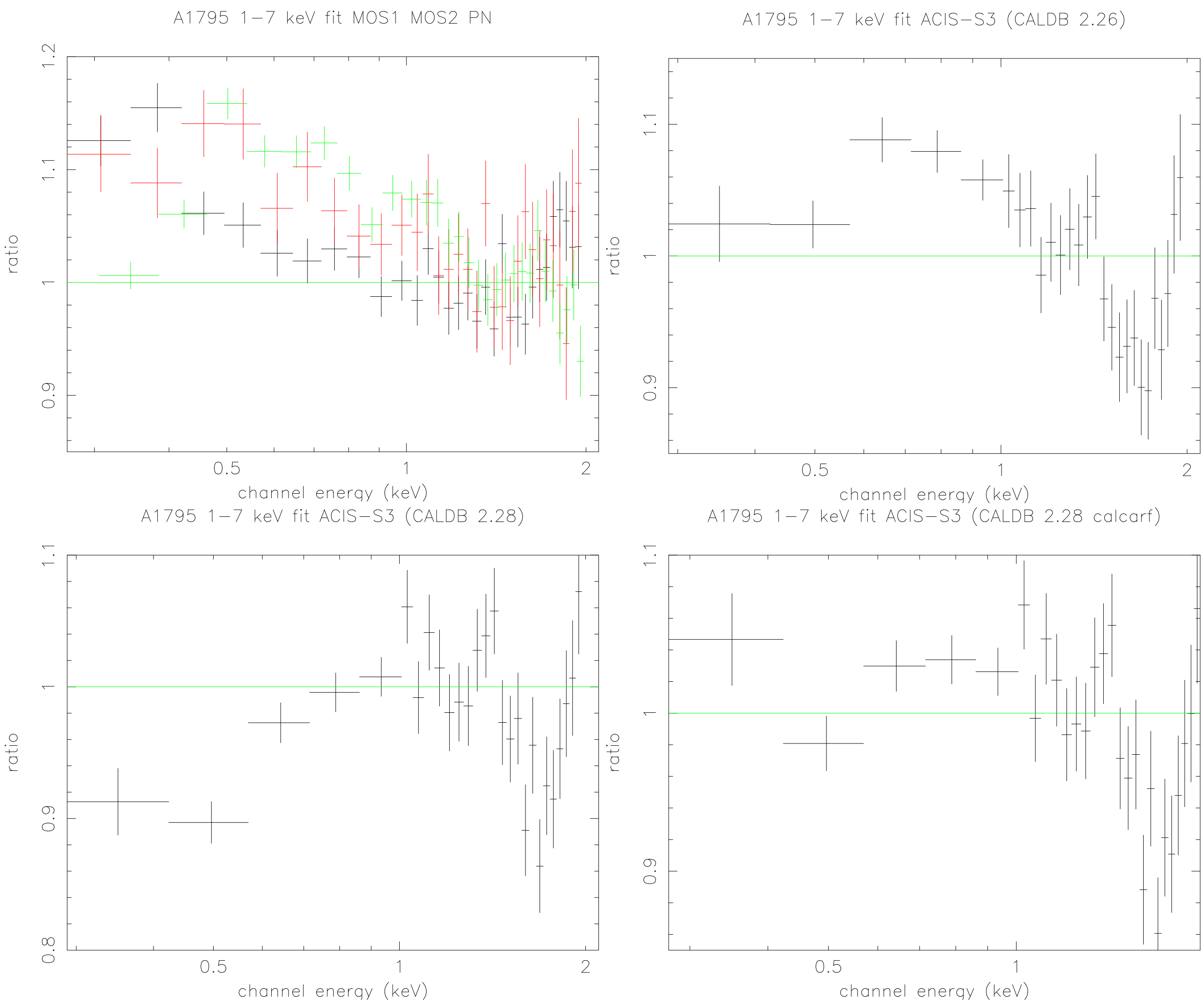

Fig. 7.— A1795, 1-7 keV fit results

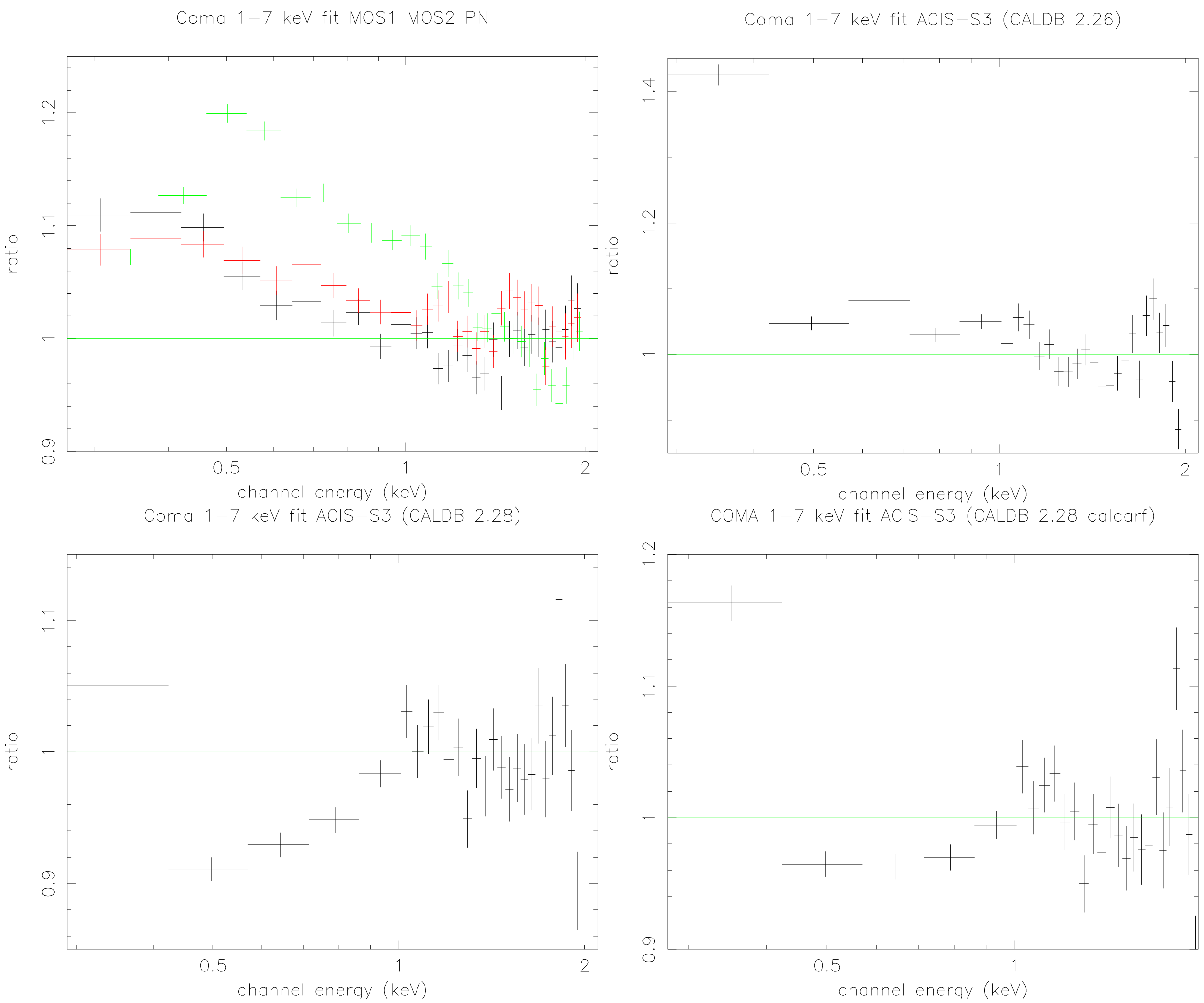

Fig. 8.— Coma cluster, 1-7 keV fit results

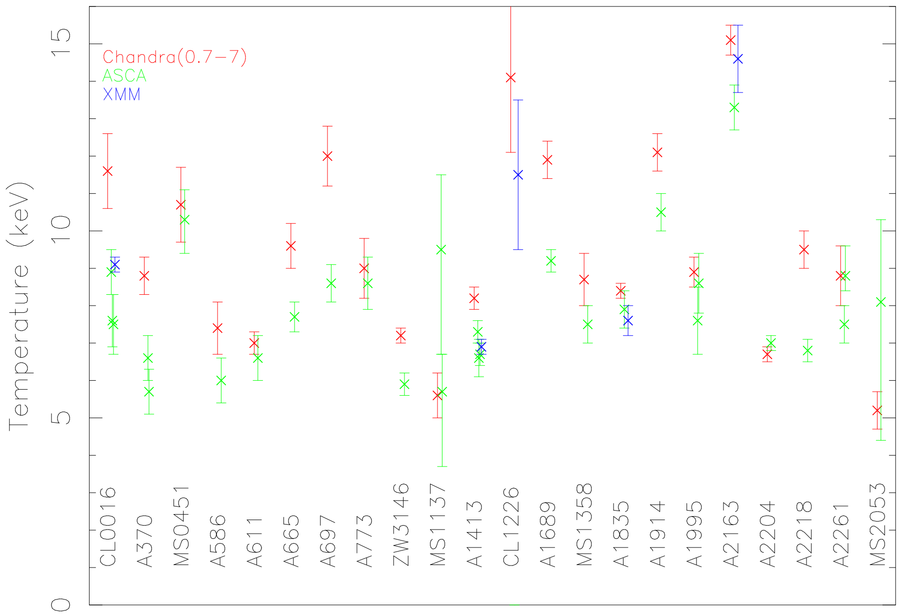

Fig. 9.— Comparison of Chandra, ASCA and XMM temperatures

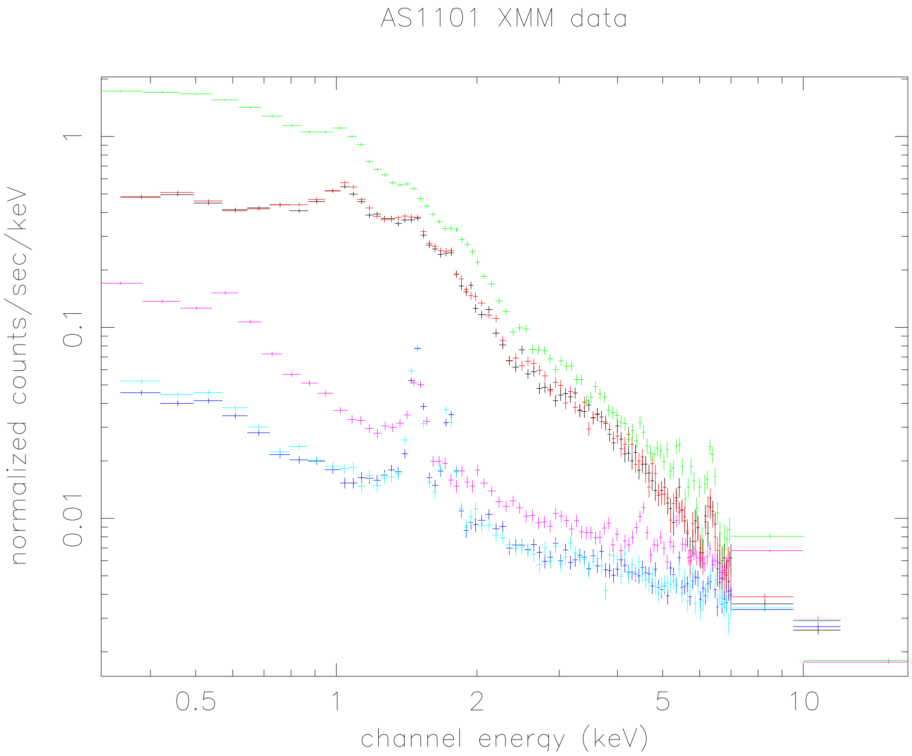

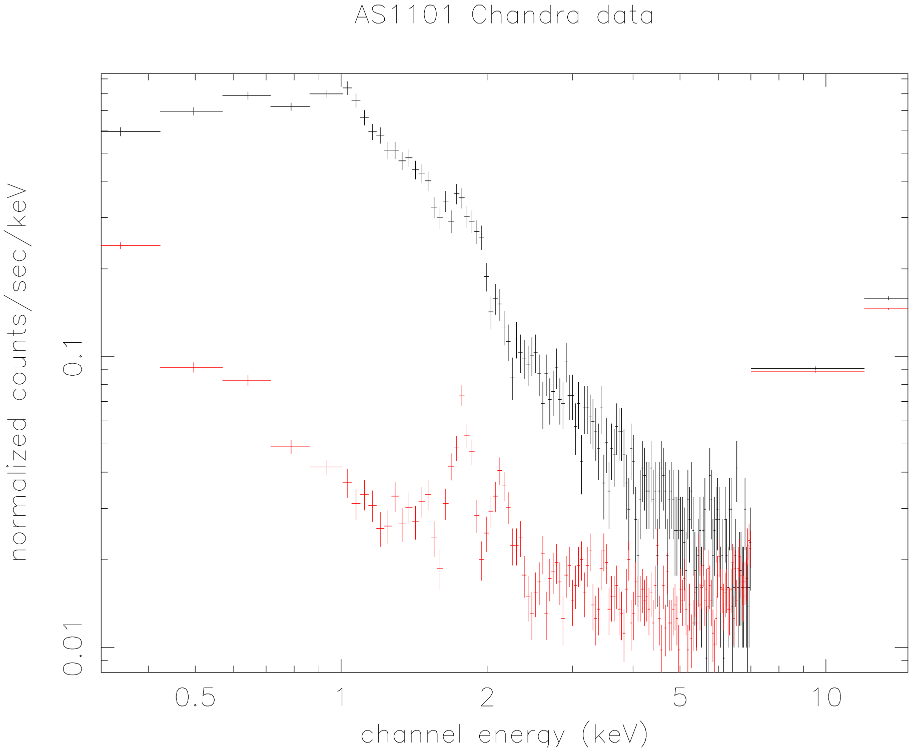

Fig. 10.— AS1101 data with background

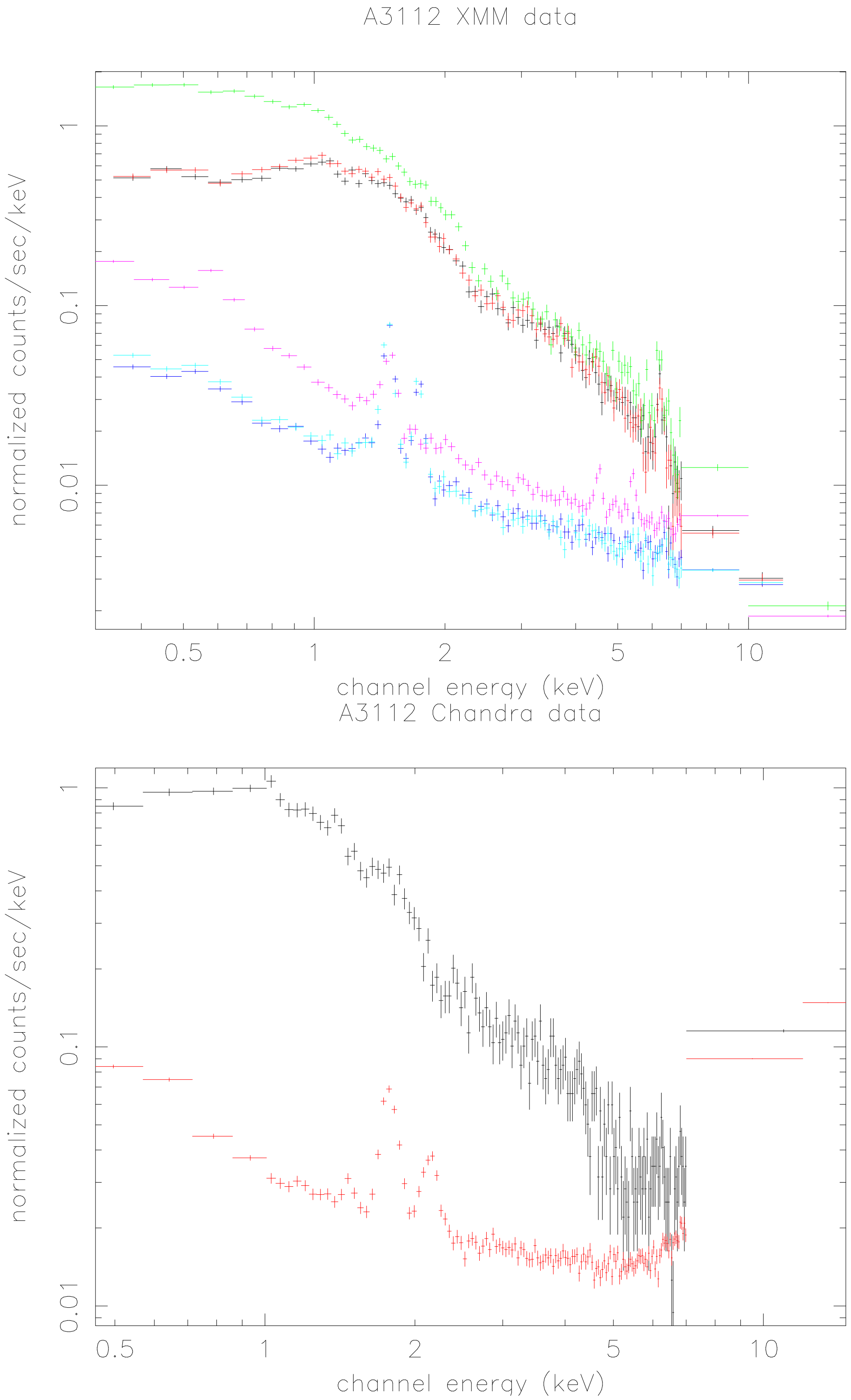

Fig. 11.— A3112 data with background

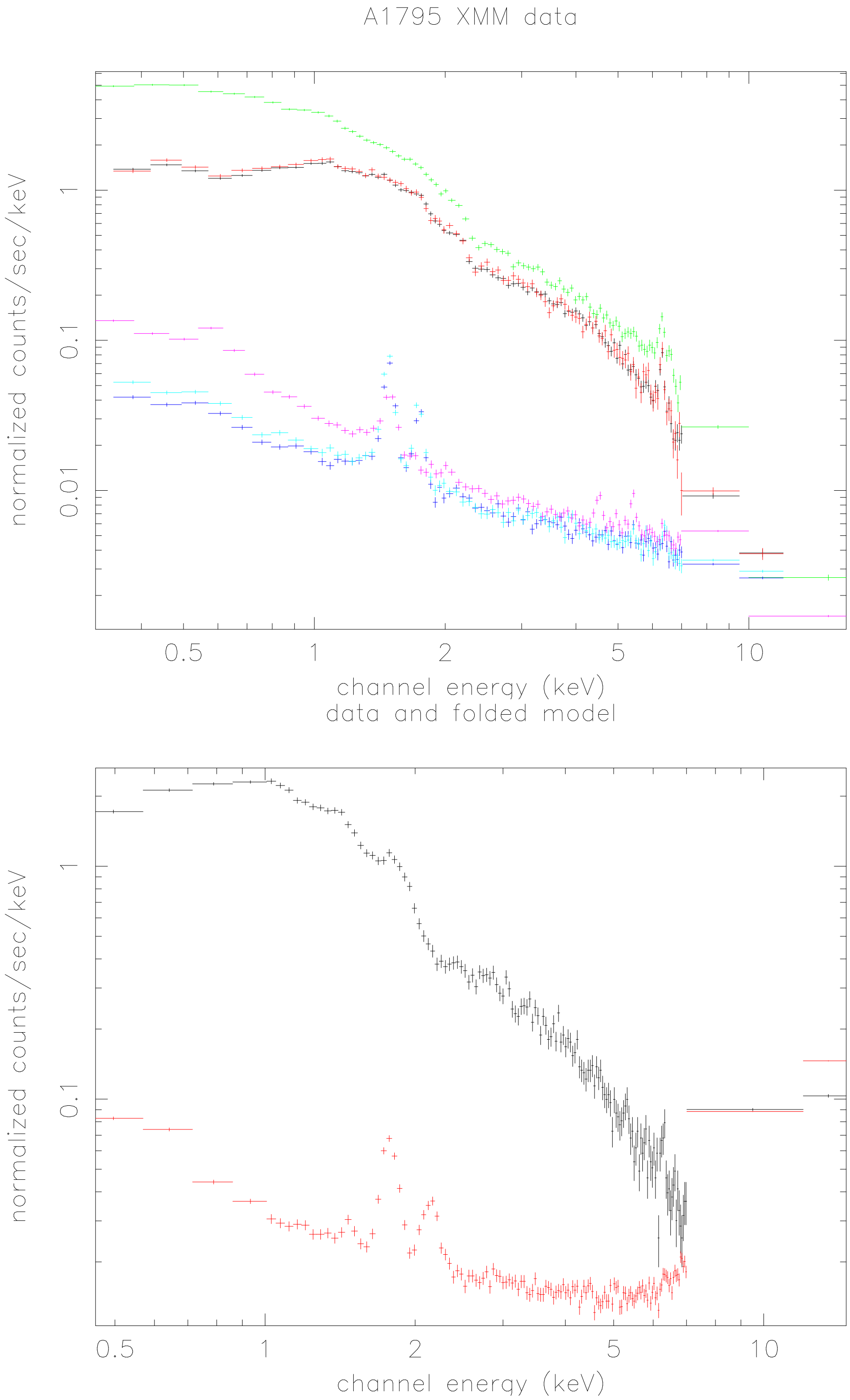

Fig. 12.— A1795 data with background

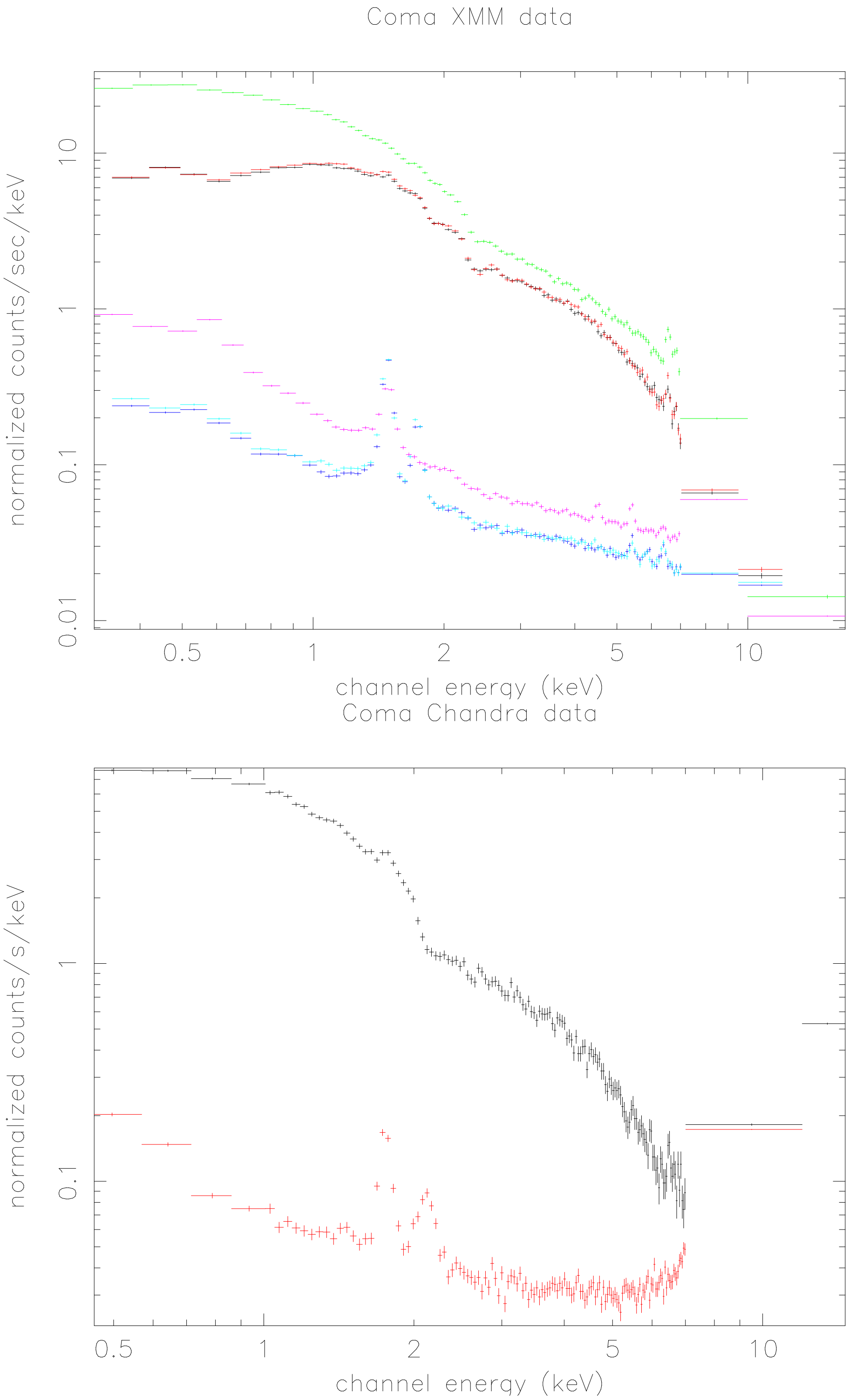

Fig. 13.— Coma data with background

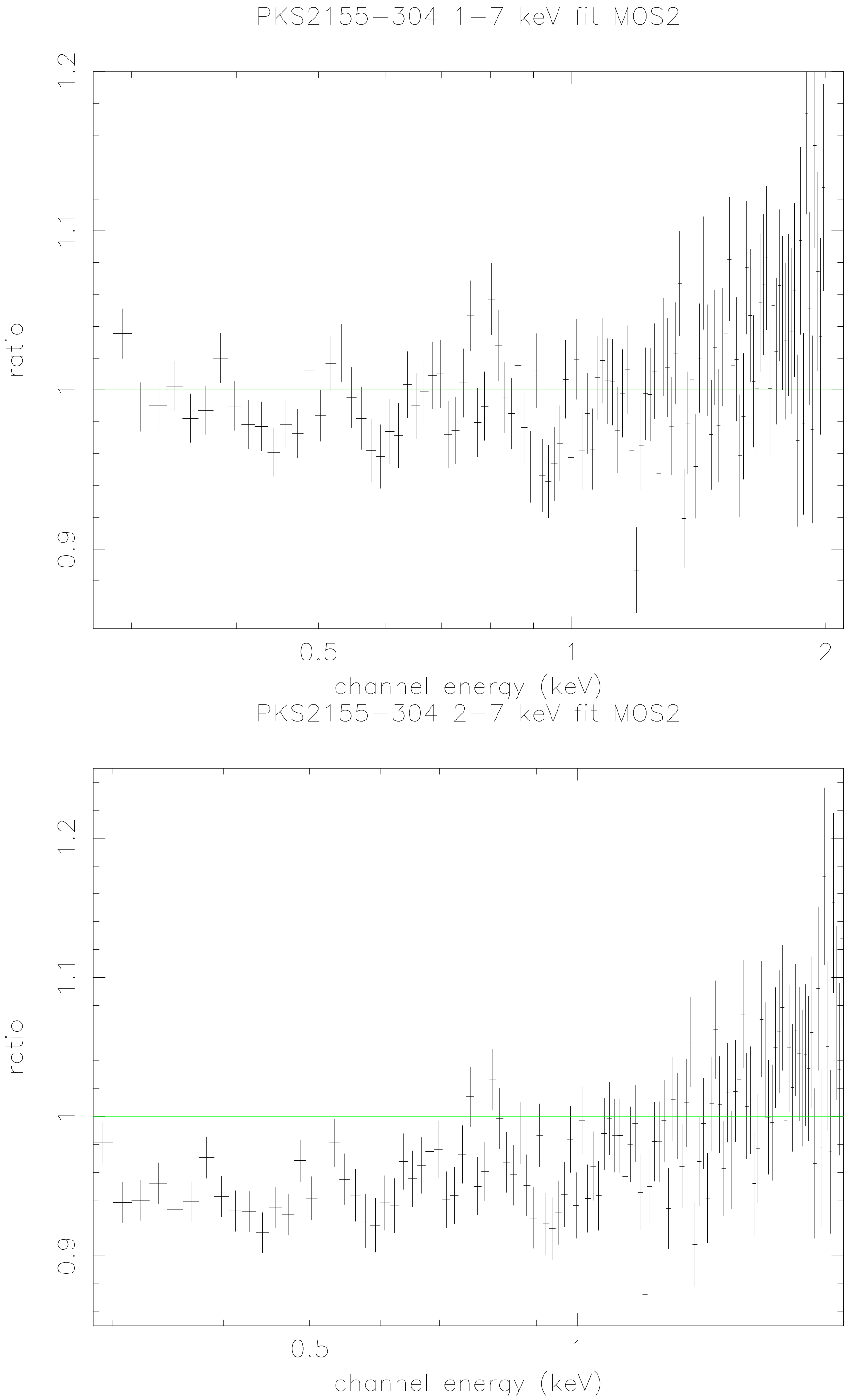

Fig. 14.— PKS2155-304 residuals, MOS2 only fit

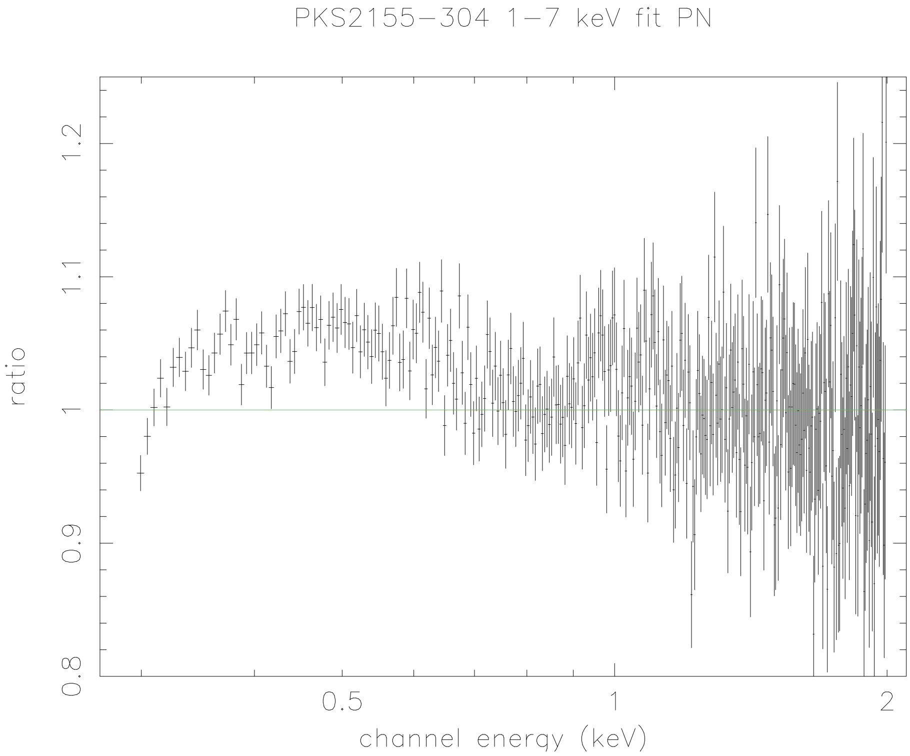

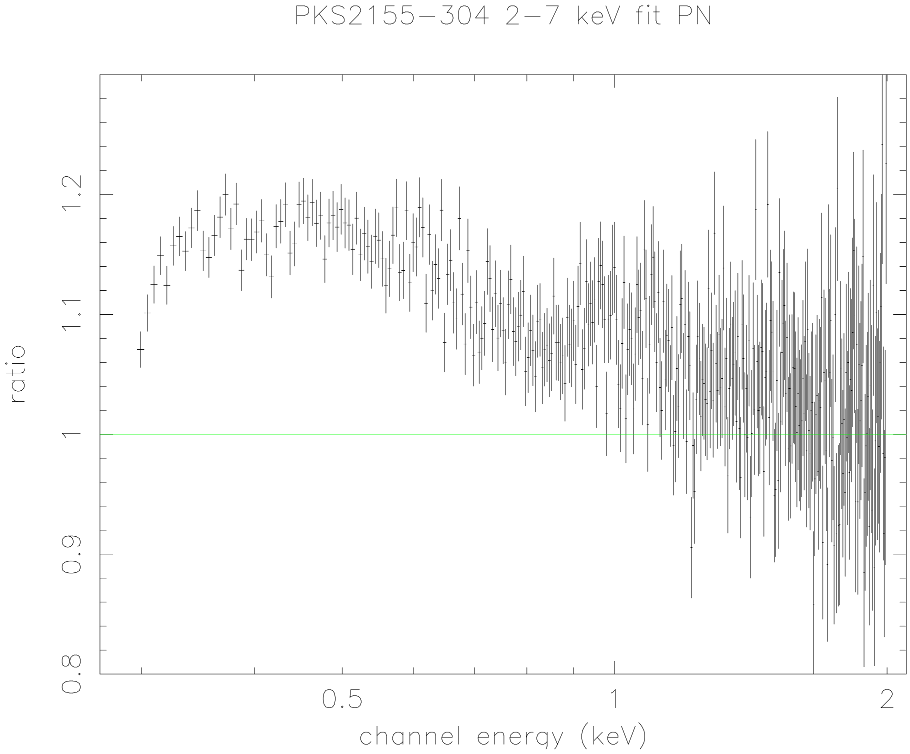

Fig. 15.— PKS2155-304 residuals, PN only fit

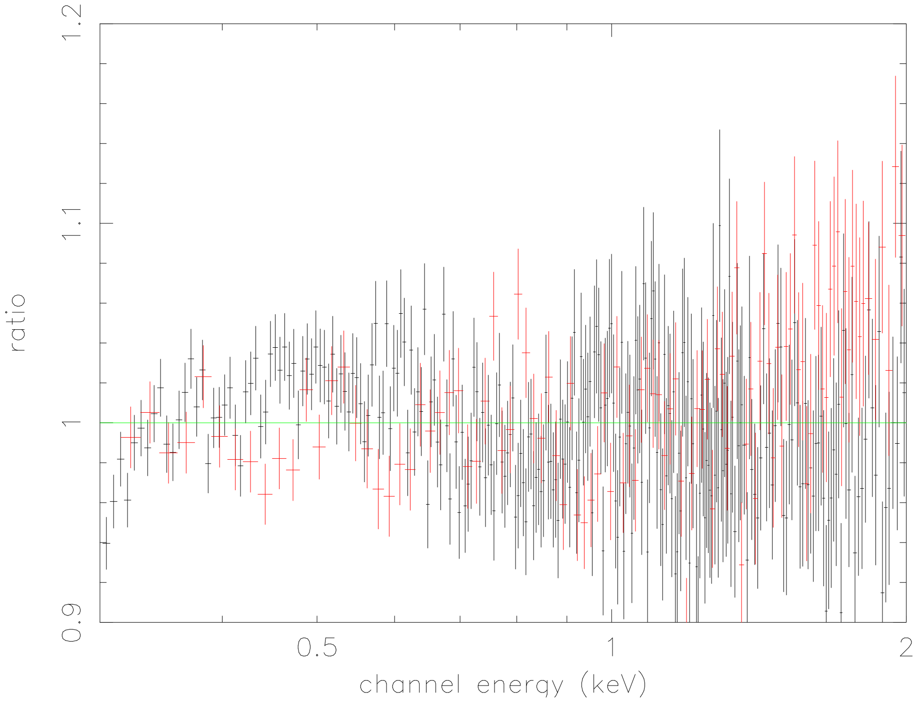

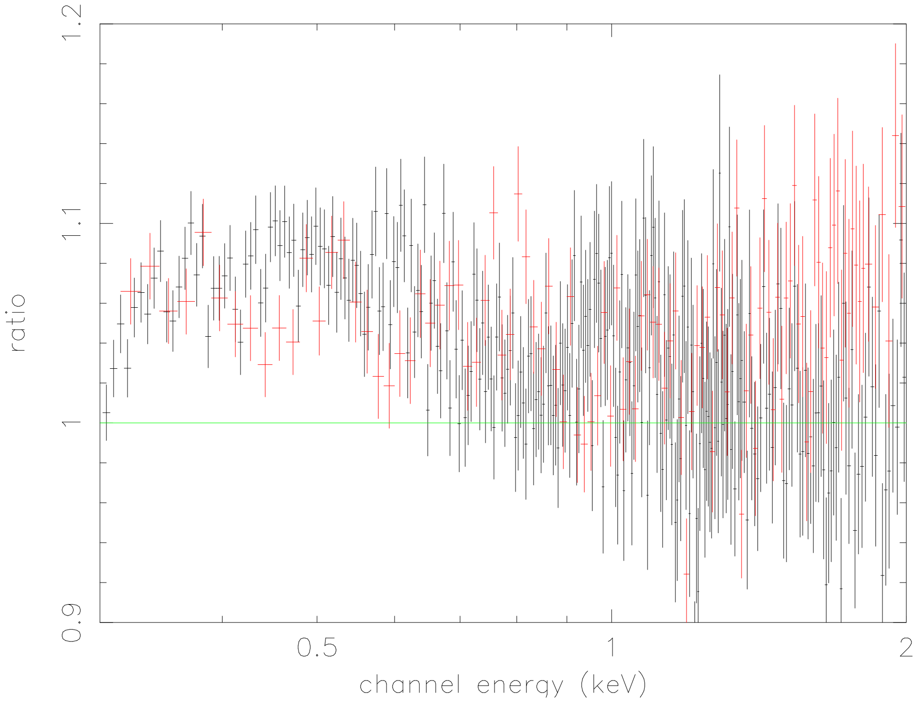

Fig. 16.— PKS2155-304 residuals, joint MOS/PN fit. (a) Low-energy residuals of the 0.3-7 keV power-law model of PKS2155-304. (b) Residuals of the 2-7 keV power-law model of PKS2155-304. In black is the PN data and in red the MOS2 data.